Prestack v(z) f-k migration images for Blackfoot III 2D multi-component data: an update

Xinxiang Li, Gary F. Margrave and Colin C. Potter

ABSTRACT

This paper shows some updated images from Blackfoot III 3C-2D data. The images from the vertical-component data with highly focused target sand-channel tie very well with the synthetic seismograms in relative depth, even though the imaged target-depth does not exactly match the geological depth. As for the images from the radial-component data, the updated images have higher quality, because the results previously shown were erroneously migrated from asymptotic common conversion point (ACCP) binned radial-component data. Some quality control procedures to determine if the data has been ACCP binned are also discussed.

INTRODUCTION

The algorithms of v(z) f-k migration and its extension for prestack PP and PS seismic data were introduced by Margrave (1998) and Li and Margrave (1998). Some prestack migration images for synthetic as well as Blackfoot III (acquired in 1997) 2D multi-component data were shown in Li and Margrave (1998). The images from the synthetic data have very high quality. The images from the vertical-component of Blackfoot data were sharply focused at the target, although the imaged target-depth does not match its geological depth. Some results from the Blackfoot radial-component data were also shown, but the images are disappointing.

The computer implementation of the prestack v(z) f-k algorithm released with the 1998 CREWES research report was based on the Fourier domain nonstationary migration filters. One advantage of using Fourier domain migration filters is that the algorithm is explicitly an extension of the Stolt's f-k migration algorithm (Stolt, 1978) but with accurate accommodation of the vertical velocity variations. In addition, this implementation can be a potentially very fast algorithm as long as some efficient algorithm can be found to compute the f-k domain migration filters.

In this paper, recent analysis of the images from Blackfoot vertical and radial-component data are shown. Especially, much better converted wave images are shown. Some updated computer implementations of the prestack v(z) f-k migration algorithm are also discussed.

COMPARISON OF PP IMAGES AND SYNTHETIC SEISMOGRAMS

The v(z) f-k migrated depth section from vertical-component of the Blackfoot data velocities provides a highly focused image of the target sand-channel, but the image depth is about 200 meters too deep. Slower velocities ensuring the correct depth of the sand-channel, however, resulted in poor images (Li and Margrave, 1998). This mismatch-in-depth also happens to the best stacking velocities when they are used to convert the time sections to depth sections. An explanation may be the angle

dependence of the velocities in this area, which may be better approximated by a migration scheme for media with transverse isotropy with vertical symmetric axis (VTI) (Li et al., 1999).

In practical seismic interpretation, the relative traveltimes or depths of a set of reflection events on the stacked or migrated sections often play an important role in phase-tying the seismic with synthetic seismograms. In this aspect, the depth image obtained from the prestack v(z) f-k migration of the vertical-component Blackfoot data was compared with synthetic seismograms produced from well-log information. Figure 1 shows the result of the interpretation, where the vertical axis is the depth from the v(z) f-k image. It can be seen that the relative depths of the seismic and synthetic tie very well, except perhaps in the interior of the channel.

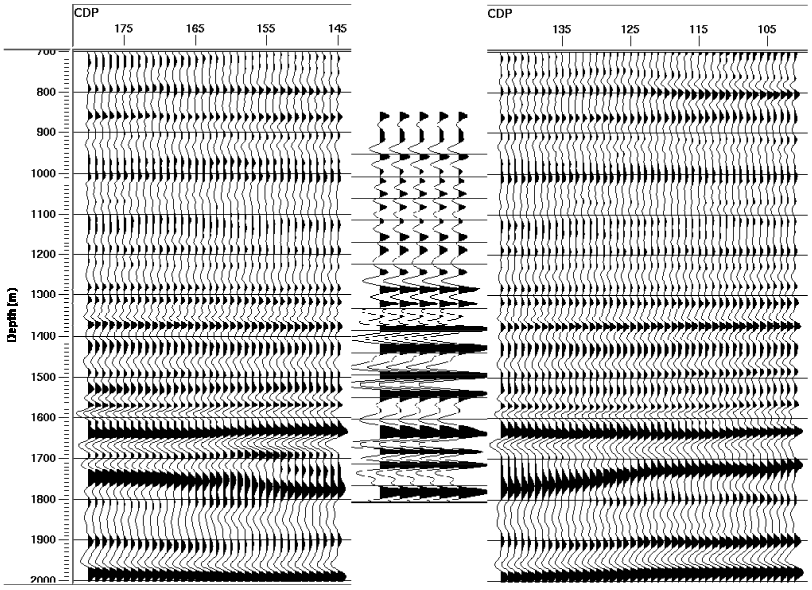

Figure 1: Phase-tie of the v(z) f-k depth section with synthetic seismogram in depth.

Another way to compare the depth section of v(z) f-k image with relevant time migration sections is to convert the depth section into time with the migration velocity. This was done in Li and Margrave (1998), and the results showed that the v(z) f-k image was preferred for its higher imaging quality than that of some poststack migration results.

PS MIGRATION INCLUDES THE COMMON CONVERSION POINT (CCP) BINNING PROCESS

The prestack v(z) f-k migration algorithm can also be used to migrate converted-wave data. Li and Margrave (1998) showed some results from its applications to some synthetic and real data. The v(z) migration is equivalent to time migration for pure-mode (PP or SS) cases, as it assumes only the vertical velocity variations. However, for mode-conversion cases (PS or SP), this algorithm cannot be directly expressed as an equivalent time migration scheme mainly because of the asymmetric ray paths of the mode converted waves.

As a prestack depth migration, v(z) f-k migration algorithm contains the depth varying common conversion point (CCP) stacking process, which is usually done by introducing a simplified CCP binning process in conventional converted-wave data processing. One essential requirement of a depth migration algorithm is accurate velocity models and, when migration velocities are known, the simplified CCP binning process is no longer needed because the accurate conversion points can be obtained through the accurate velocity information.

To show how v(z) f-k migration locates the conversion points in each depth level, the migration responses of one input trace are displayed with its relevant geometry in Figure 2. Figure 2(a) shows the migration response of the PP algorithm, and Figure 2(b) shows the response of the PS algorithm. The input trace has an absolute offset of 1,009 meters, and its CMP number is 151. The P-wave velocity and the S-wave velocity are set to constant for simplicity. As expected, the response of the PP migration consists of a series of semi-ellipses with the symmetry axis being the vertical line through the mid-point location (denoted by dashed line) and the same foci at the source (denoted as a '*') and the receiver (denoted as a 'square') locations. For flat reflectors, the reflection points at all depth levels are the points on these semi-ellipses at which the tangent lines are horizontal.

The migration response of this trace from the PS algorithm consists a series of "skewed", asymmetric semi-ellipses. As in the PP case, for flat reflectors, the P-to-S conversion point at each depth level corresponds to the point on the "ellipse" at which the tangent line is flat. The black solid curve in Figure 2(b) traces the theoretical conversion points that were computed directly from the velocity information and the trace geometry. It can be seen that the conversion points from the migration response match exactly the theoretical conversion points. As comparisons, the asymptotic CCP location, which does not change in depth, is plotted as a white vertical line, and the CMP location is shown as the dashed dark line.

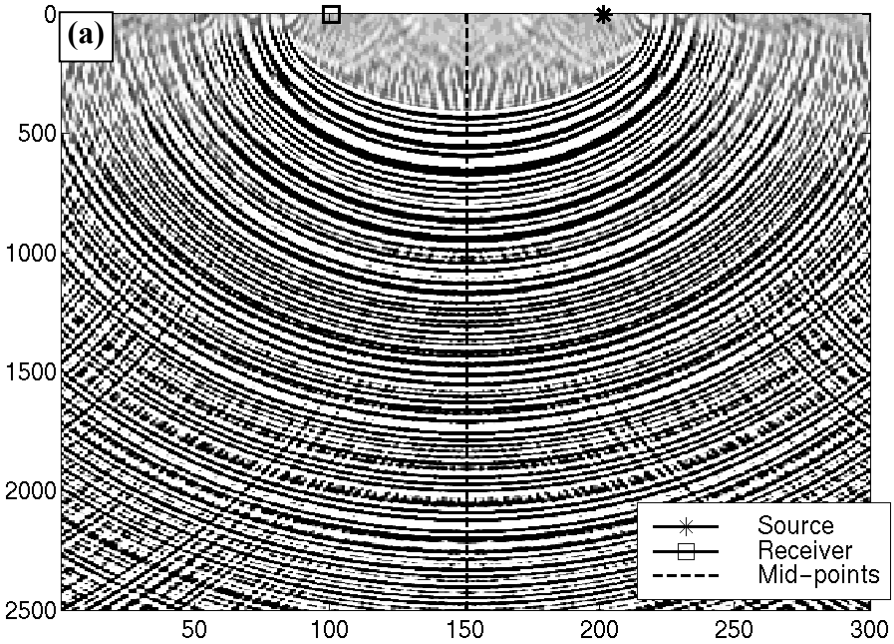

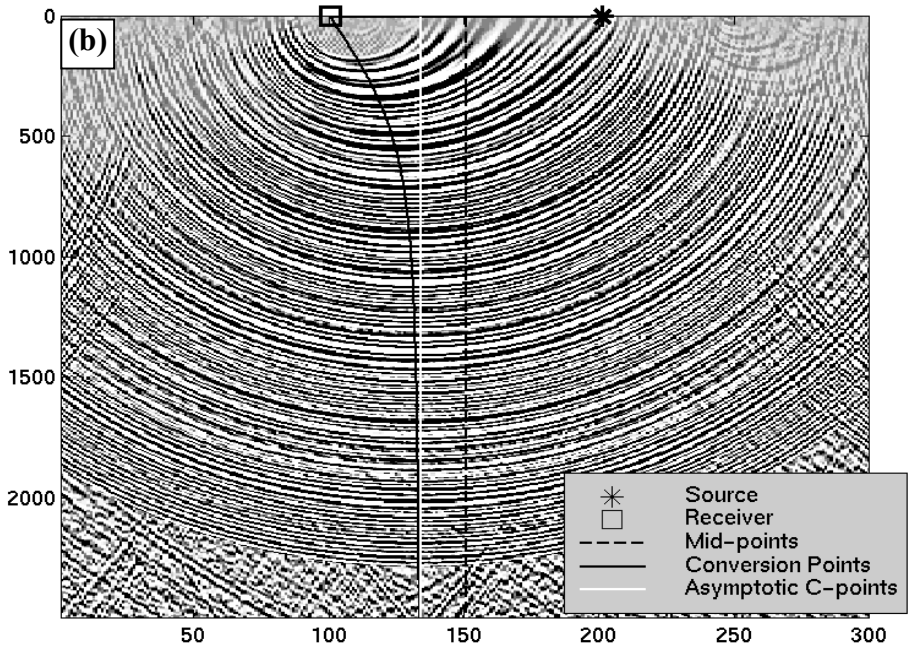

Figure 2: The migration responses from one input trace with (a) from the PP algorithm and (b) from the PS algorithm of v(z) f-k migration algorithm.

VERIFYING THAT CCP BINNING HAS OCCURED

The converted-wave (radial and transverse components) data are almost always acquired with the same or similar geometry as the vertical-component data. This provides some convenient ways to verify if a set of converted-wave data is CCP binned or not. This is important practically, because most of the conventional converted-wave data processing flows include the CCP binning process, and many prestack migration and/or DMO algorithms are more suitable for data before binning. The binning algorithms do not change the source and receiver information of recorded traces, but often change the CDP information in the trace headers and/or in the databases (such as the module "P-S asymptotic binning" in ProMAX). If a prestack algorithm uses CDP information, it is necessary to know if the trace header and database information is appropriate. There are many ways to check if the data is CCP binned or not. Two methods are stated here. They work for ProMAX 2D and could be used in general.

CDP fold distribution

The data after ACCP binning usually have different CDP fold distributions. If the geometries of the acquisition of the vertical and radial data are the same, it is convenient to display the CDP fold in both the vertical line database and the radial line database. If they are different, the radial data should have been CCP binned already; if they are the same, then the radial data have not been binned yet. Figure 3(a) shows the CDP fold of the vertical-component data from Blackfoot III 2D, which is the same as the radial data before CCP binning, and Figure 3(b) shows the CDP fold after ACCP binning in the radial line database.

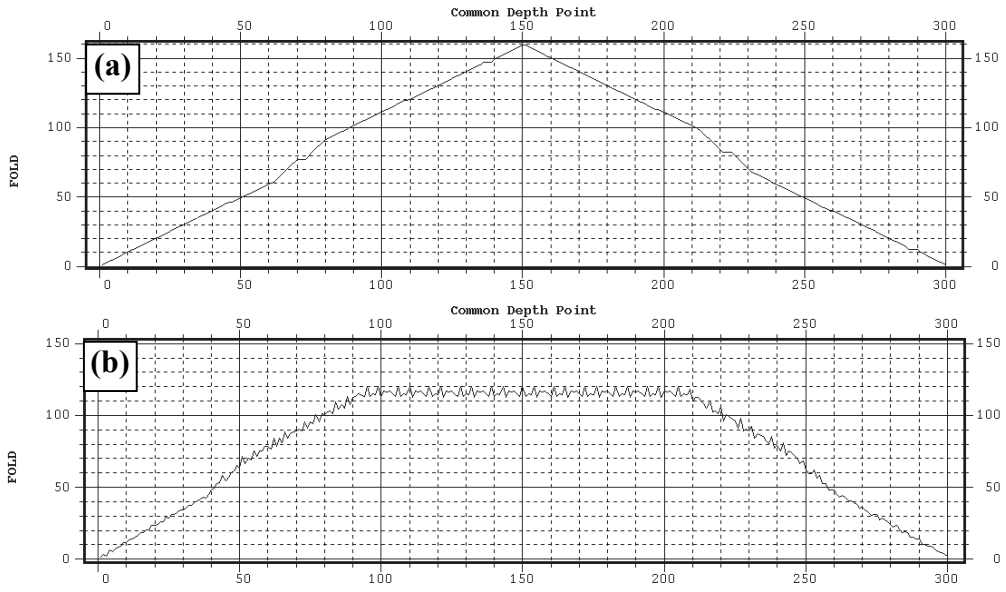

Figure 3: CDP fold distributions before (a) and after (b) ACCP binning.

If there is no PP geometry available, or the PP geometry is different, simply displaying the CDP fold of the radial data can also help. It can be seen from Figure 3 that, the fold curve in Figure (a) is stable and "smooth", the fold curve in Figure 3(b), however, is not "smooth". This non-smoothness indicates that the data may have been CCP binned. Eaton and Lawton (1992) and Li and Lu (1999) explained some reasons why the CCP binned folds are not smooth.

CDP numbers in shot gather

Another simple way to identify the CCP binning process is to display a shot gather from the PP data and one from the PS data at the same shot location, and both with CDP number as the header notations. When the acquisition geometries for both datasets are the same, the CDP notations on both displays should be the same if the radial data have not been CCP binned. If the radial data is CCP binned, the CDP notations will be different. Two shot gathers with the same FFID (field file ID number) are shown in Figure 4, where (a) shows the gather from the vertical-component data and (b) shows the gather from radial-component data after ACCP binning. The CDP ranges of the two gathers are different. That is: the CDP range of this shot gather is from No. 54 to No. 200 before binning, and the CDP ranges from No. 35 to No. 240 after binning.

Again, if the PP data is not available or the acquisition geometries are different, only displaying the PS data can also help. Check the increments of the CDP notations between traces in a shot gather, if the increments change (usually larger for larger offsets) along the display, the data should have been CCP binned. If the CDP number increment keeps the same from trace to trace, this data may not have been binned.

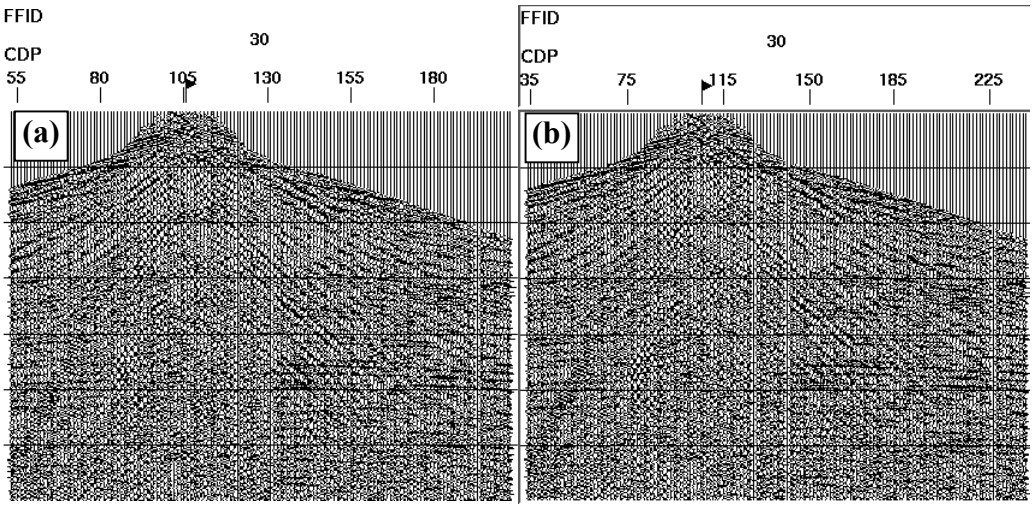

Figure 4: The same shot gather before (a) and after (b) ACCP binning with CDP number as the trace notation. Note that the CDP ranges for the two displays are different.

IMAGES FROM THE CONVERTED-WAVE DATA

The migration results from the Blackfoot radial-component data shown in Li and Margrave (1998) do not have good images. The main reason is that the input data to the migration processes were already ACCP binned and the CDP information in the database and trace headers were changed. Thus, after migration, the data was CCP binned twice. As a result, the shift from mid-points to CCPs is too large. For comparison, the old results of v(z) f-k migration from negative offset traces and positive offset traces are shown in Figure 5, the correct migration results are shown in Figure 6.

The traces of the input data are equalized, so the amplitudes of the images in Figure 5 and Figure 6 approximately reflect the CCP fold distributions. It is expected that the energy on traces with negative offset will be moved to smaller surface-location-number direction (to the right in these displays), and the energy on the positive-offset traces will be moved to larger surface-location-number direction (to the left in these displays). These lateral shift limits are shown schematically with white lines in Figure 5 and Figure 6. The shift limits in Figure 5 are larger in extents (and they are incorrect) compared with those in Figure 6. The white lines in Figures 5 and 6 can be considered as the shift limits in the receiver directions, it can be seen that the white lines in Figure 5 are much closer to the boundaries of the sections than the ones in Figure 6.

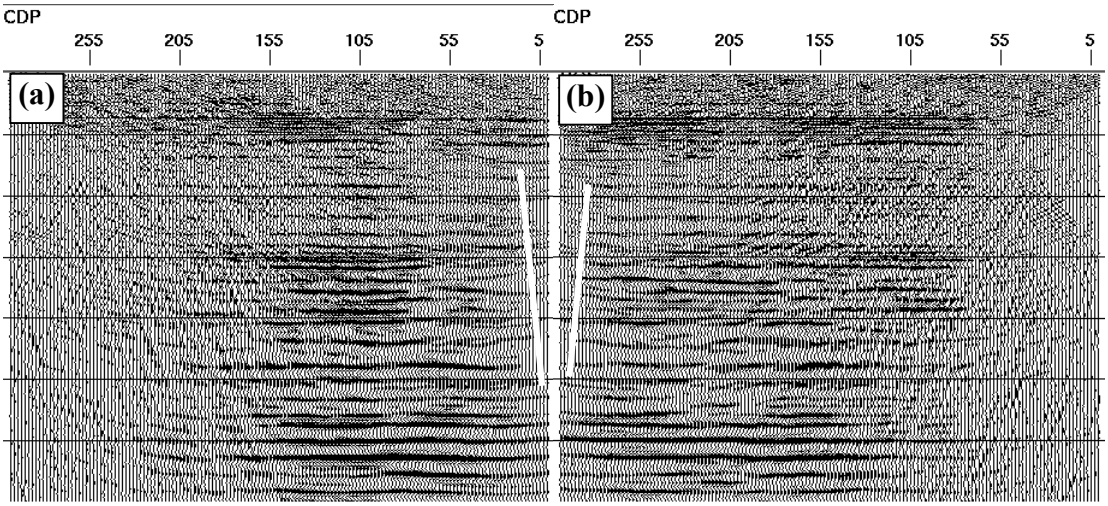

Figure 5: Migration results from ACCP binned data, where (a) is from the negative offset traces and (b) is from the positive offset traces.

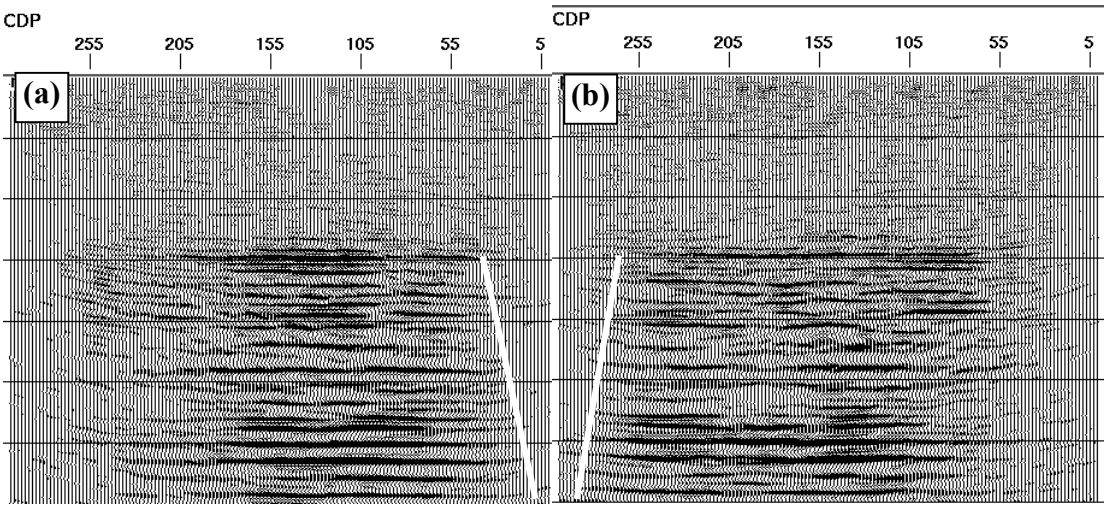

Figure 6: Correct migration images from (a) the negative offset traces and (b) the positive offset traces of the Blackfoot 2D radial-component data.

The correct migration results provide much better images. The detailed images of the target sand-channel area are shown in Figure 7 and Figure 8. The images in Figure 7 (a) and (b) are portions of Figure 5 (a) and (b), respectively, and the images in Figure 8(a) and (b) are portions of Figure 6(a) and (b), respectively. Both the signal-to-noise ratio and the resolution of the images in Figure 8 are better than those in Figure 7. The channel on the images should be between 1700 to 1800 m, as indicated in Figure 8(a) by two black arrows.

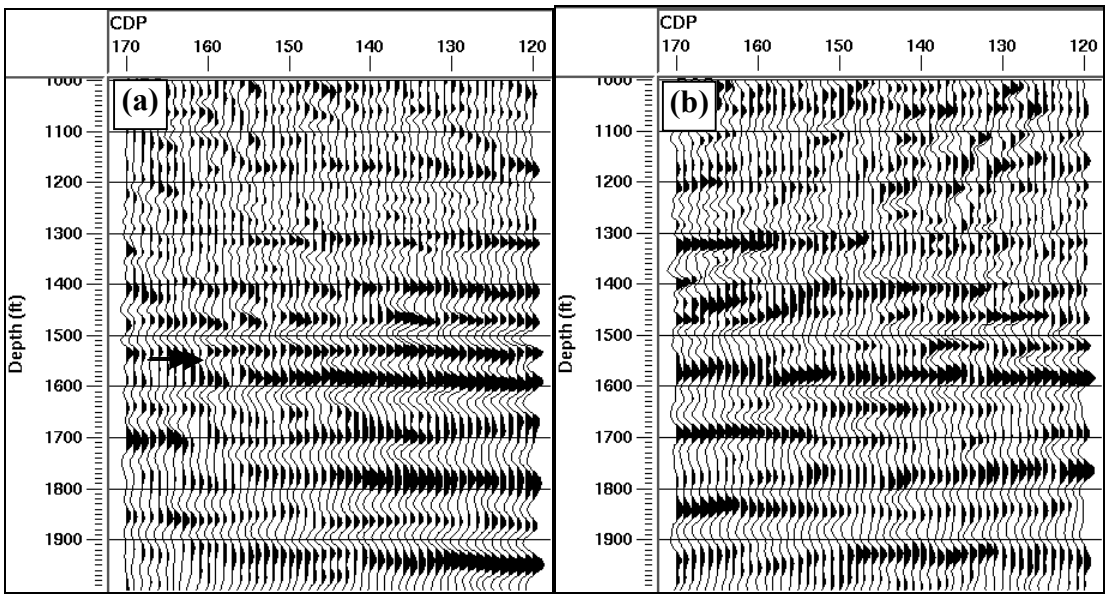

Figure 7: The target sand-channel portions of the images shown in Figure 5, where (a) is a portion of Figure 5(a) and (b) is the corresponding portion of Figure 5(b).

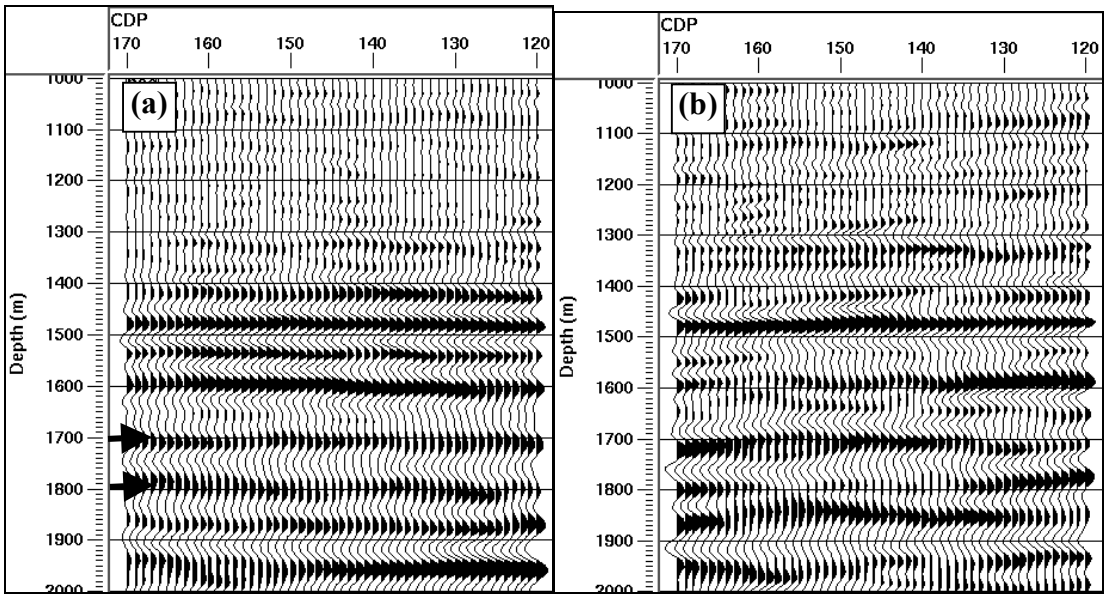

Figure 8: The target sand-channel portions of the images shown in Figure 6, where (a) is a portion of Figure 6(a) and (b) is the corresponding portion of Figure 6(b).

The final radial-component data image is the summation of the images migrated from the negative-offset data and the positive-offset data. Figure 9 shows a portion of the final image (converted to time) with the sand-channel target included. The sand-channel Glauconitic top is interpreted between 1600 ms and 1700 ms as indicated by the arrows. One synthetic seismogram is inserted at the corresponding well location. The major events above the Glauconitic top in the image tie very well with the synthetic. One reason why the events below the Glauconitic top do not tie well is that the shear sonic logs from below the sand-channel is not available, and for producing a longer synthetic seismogram, shear log information from another well in this area was padded.

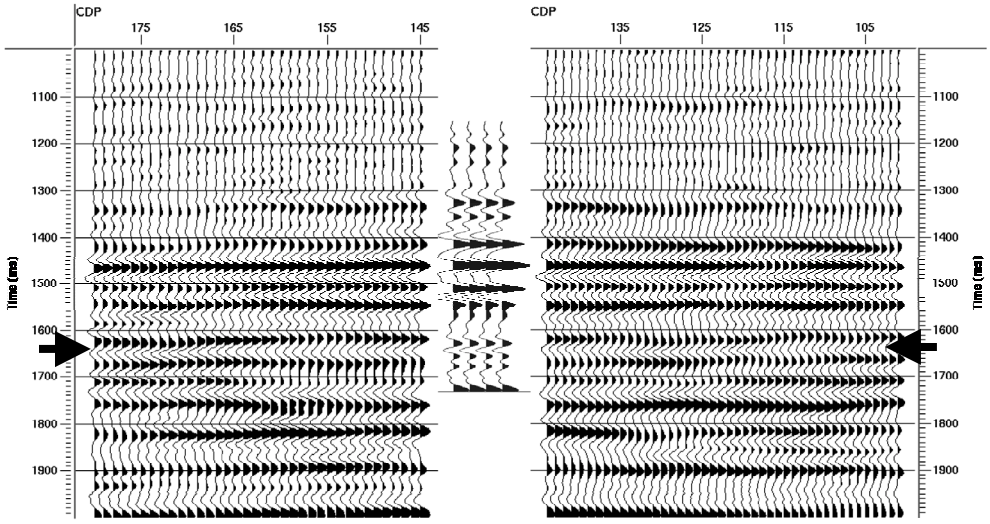

Figure 9: The radial-component image the sand-channel target with synthetic seismogram inserted at the corresponding CDP location.

MIXED DOMAIN ALGORITHM AND OTHER UPDATES

The computer implementation of the v(z) f-k migration is also updated. The results shown in Li and Margrave (1998) were obtained using the migration filters computed in Fourier domain, and at that time, the mixed-domain algorithm had not been implemented. Because the mixed-domain migration filters take less time to compute by the accurate formulas shown in Li and Margrave (1998), the new implementation of the prestack v(z) f-k migration module in ProMAX 2D contains the mixed-domain algorithm. This mixed-domain filter method does take less time in computation, although mathematically these two algorithms are exactly the same.

The prestack v(z) f-k migration algorithm is also extended to schemes for migration from separated common offset sections, (Li and Margrave, 1999b) and migration for VTI media (Li et al.,1999). The details are written as separate reports in this volume.

CONCLUSIONS

The prestack v(z) f-k migration algorithm can produce high quality migration images for both PP and PS seismic data. The new implementation also includes the mixed-domain migration filter computation and application, which forms a slightly faster algorithm.

The v(z) f-k migration process includes the conversion point binning and stacking processes automatically, and it should be ensured that the input converted-wave data has not been CCP binned.

ACKNOWLEDGEMENTS

The authors would like to thank the sponsors of CREWES Project for their financial support. Discussions with Ms. Han-Xing Lu and Mr. Chuandong (Richard) Xu have been very helpful.

REFERENCES

Eaton, D. W. S. and Lawton D. C., 1992, P-SV stacking charts and binning periodicity, Geophysics, 57, 745-748.

Lawton, D. C., 1993, Optimum bin size for converted-wave 3-D asymptotic mapping, CREWES Research Report, Vol. 5, Ch 28.

Li, X. and Margrave, G. F., 1998, Prestack v(z) f-k migration for PP and PS data, CREWES Research Report, vol. 10.

Li, X. and Margrave, G. F., 1999a, Prestack v(z) f-k migration for PP and PS seismic data, 69th SEG Annual Meeting, Expanded Abstract.

Li, X. and Margrave, G. F., 1999b, Prestack v(z) f-k migration from common-offset sections, CREWES Research Report, this volume.

Li, X, Margrave, G. F. and Ferguson, R. J., 1999, Prestack v(z) f-k migration for VTI media, CREWES Research Report, this volume.

Li, X. and Lu, H.-X., 1999, A re-visit to the fold discontinuity after ACCP binning, CREWES Research Report, this volume.

Margrave, G. F., 1998, Direct Fourier migration for vertical velocity variations, CREWES Research Report, vol. 10. Ch. 36